

Microscopic model for enhanced dielectric constants in low concentration SiO₂-rich noncrystalline Zr and Hf silicate alloys

G. Lucovsky^{a)}

Departments of Physics, Electrical and Computer Engineering, and Materials Science and Engineering,
North Carolina State University, Raleigh, North Carolina 27695-8202

G. B. Rayner, Jr.

Department of Physics, North Carolina State University, Raleigh, North Carolina 27695-8202

(Received 24 July 2000; accepted for publication 1 September 2000)

Dielectric constants, k , of Zr(Hf) silicate alloy gate dielectrics obtained from analysis of capacitance–voltage curves of metal–oxide–semiconductor capacitors with 3–6 at. % Zr(Hf) are significantly larger than estimates of k based on linear extrapolations between SiO₂ and compound silicates, Zr(Hf)SiO₄. Analysis of infrared spectra of Zr silicate alloys with 3–16 at. % Zr indicates increases in the coordination of Zr to O atoms from 4 to approximately 8 with increasing Zr content. The major contributions to enhancements in k in these low Zr(Hf) content alloys are explained by a transverse infrared effective charge that scales *inversely* with increasing Zr–O bond coordination.
© 2000 American Institute of Physics. [S0003-6951(00)01344-9]

There is considerable interest in replacement dielectrics for SiO₂ in metal–oxide–semiconductor (MOS) devices with channel lengths <100 nm. Scaling requires a gate dielectric capacitance *equivalent* to a SiO₂ thickness of <1.5 nm, a regime where direct tunneling exceeds 1–5 A/cm² at operating biases, and is too high for many mobile applications.¹ Insulators with higher dielectric constants offer potential for increased capacitance in physically thicker films, providing a possible way to reduce direct tunneling.² MOS capacitors with SiO₂-rich Zr and Hf silicates with 3–6 at. % Zr(Hf) have been reported to have increased dielectric constants and reduced tunneling currents.^{1,3–5} Reported values of k from capacitance–voltage curves are ~8–11, and more than 50% larger than values estimated from a linear extrapolation of k between SiO₂, ~3.9, and the compound silicates, ~12 (Fig. 1). These *enhanced* values of k can not be reconciled with macroscopic dielectric theory that predicts a downward bowing between end members in a mixed materials system.⁶ Since macroscopic theory applies to mixtures in which chemical bonding of constituents does not change with composition, it is important to determine if SiO₂-rich Zr(Hf) silicate alloys satisfy this condition.

Chemical bonding in Zr silicates ([ZrO₂]_x[SiO₂]_{1-x}) has been studied by Fourier-transform infrared spectroscopy, (FTIR);⁷ similar bonding is expected in Hf silicates. Figure 2 displays absorbance for Zr silicate films prepared by remote plasma enhanced chemical vapor deposition.^{2,7} Alloy compositions were determined to ±0.05 by Rutherford backscattering spectrometry. Spectra of as-deposited films and films annealed for 30 s in Ar at temperatures to 800 °C (not shown) are essentially the same, whereas spectra of films annealed at 900 °C are markedly different. Features in as-deposited films with $x \sim 0.1$ and 0.23 are assigned to Si–O–Si groups in *corner-connected* arrangements, as stretching modes at ~1150, 1065, and 810, and a rocking mode at

~450 cm⁻¹.^{7,8} Two other features are assigned to Si–O–Zr stretching vibrations, a terminal Si–O mode at ~950 cm⁻¹ that is a shoulder on the 1065 cm⁻¹ absorption, and a broader Zr–O feature at ~450 cm⁻¹ that is *accidentally* degenerate with the Si–O–Si rocking mode. Since both stretching modes involve predominantly O-atom motion, their frequencies reflect a significantly smaller force constant for the Zr–O vibration. This results from a Zr–O bond length of 0.22 nm compared to ~0.16 nm for Si–O.⁹ Far-IR spectra to 50 cm⁻¹ show no additional features. Spectral features in an as-deposited $x \sim 0.5$ film are assigned to a random close packing of Zr⁴⁺ and SiO₄⁴⁻ ions.^{7,8} The 800–1200 cm⁻¹ band includes SiO₄⁴⁻ vibrations, and the ~450 cm⁻¹ band is dominated by Zr–O vibrations. After a 900 °C anneal, spectral changes at all compositions indicate a chemical phase

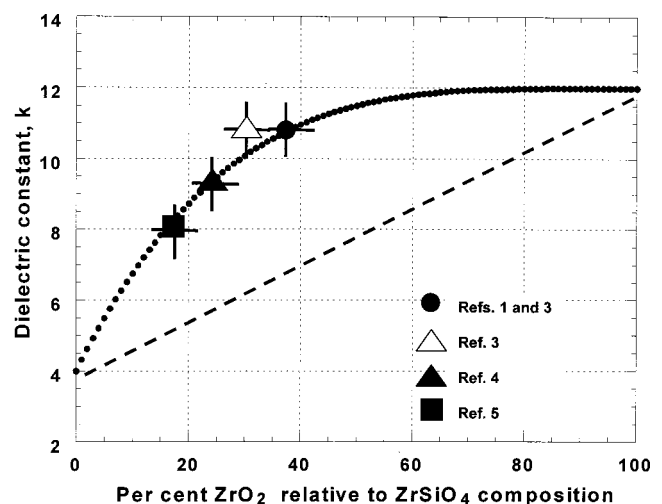


FIG. 1. The dotted curve indicates the dielectric constant calculated from Eq. (3) as a function of the percent Zr(Hf)O₂ relative to the stoichiometric silicate compound composition, Zr(Hf)SiO₄. Experimental points are from Refs. 1, 3, 4, and 5. The dashed line is a linear extrapolation between the dielectric constant of SiO₂ and a nominal dielectric constant of 12 for Zr(Hf)SiO₄.

^{a)}Electronic mail: gerry_lucovsky@ncsu.edu

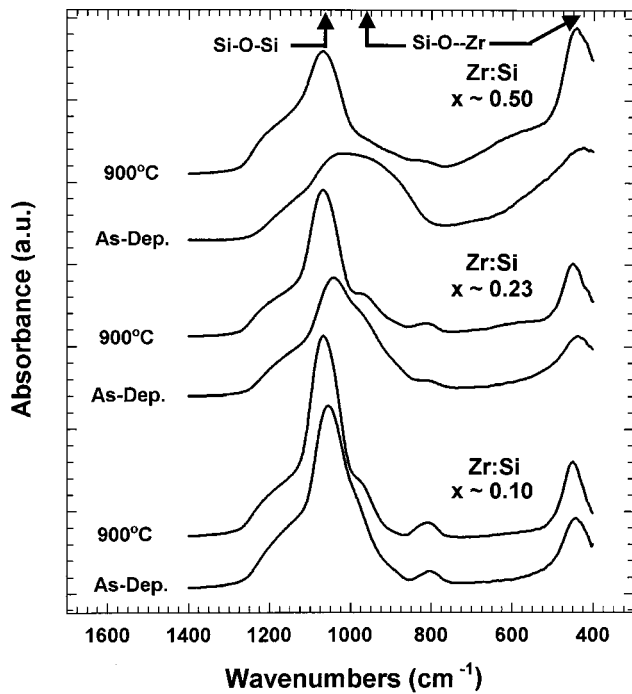


FIG. 2. Absorbance vs wave number for three Zr silicate alloys with different ratios of Zr:Si, as-deposited and after a 30 s, 900 °C anneal in Ar.

separation into (i) a noncrystalline low Zr-content silicate alloy with ~1–2 at. % Zr and (ii) noncrystalline ($x \sim 0.1$ and ~ 0.23) or crystalline ZrO_2 ($x \sim 0.5$).⁷

As in bulk silicate glasses, introduction of oxides of electropositive Zr(Hf) atoms into SiO_2 results in a breakup or *modification* of the network structure.^{10,11} Homogeneity in bulk silicate glasses quenched from high temperatures is limited by chemical phase separation, and in many instances homogeneous glasses are obtained only at relatively low metal oxide content, <5–10 mol %. This is not a limitation in thin film silicates deposited at temperatures <500 °C.^{1–5,7} The analysis below applies to these films, as well as those prepared at low temperatures, and subsequently processed at temperatures <800 °C. Capacitors with Zr(Hf) silicate dielectrics in Refs. 1, 3, 4, and 5 meet these temperature constraints. Introduction of a Zr(Hf)O_2 molecule into the SiO_2 network is assumed to break two Si–O bonds,¹¹ so that the concentration of terminal Si–O terminal bonds is linear in Zr composition. The coordination of silicon to oxygen remains 4, and there are five tetrahedral groups with different distributions of O atoms that are (i) connected to the network through *bridging* Si–O–Si bonds, or are (ii) in *terminal* Si–O groups. Figure 3 gives the fractional concentrations of these groups in Zr(Hf) silicates alloys as a function of composition as obtained from the following expression:

$$(w+z)^4 = w^4 + 4zw^3 + 6z^2w^2 + 4z^3w + z^4 = 1, \quad (1)$$

where w is the fraction of bridging O atoms, and $z = 1 - w$ is the fraction of terminal O atoms.

In alloys with $x < 0.1$, Zr atoms (or Zr^{4+} ions) are incorporated predominantly as network modifiers with four terminal negatively charged O-atom neighbors in *corner-connected* arrangements¹¹ (Fig. 4). As the mole fraction of ZrO_2 is increased, an increasing fraction of these groups have two or more terminal Si–O bonds. This causes the co-

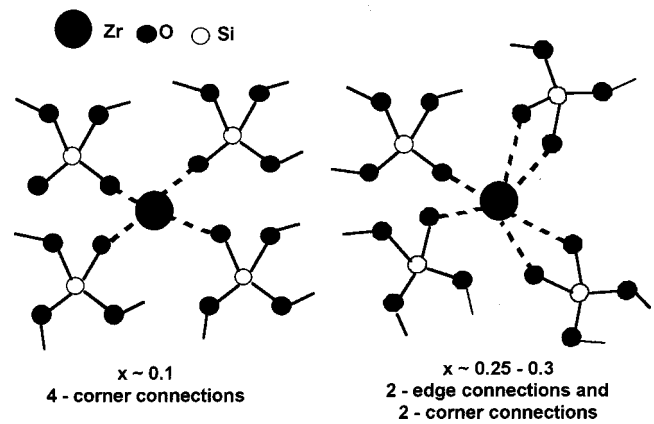


FIG. 3. Relative fractions of five tetrahedral silicon-oxygen bonding groups with different numbers of bridging and terminal oxygen atoms plotted as a function of the percent of Zr(Hf)O_2 relative to the stoichiometric silicate compound composition, Zr(Hf)SiO_4 .

ordination of Zr atoms to increase above 4 including both *edge-* and *corner-connected* arrangements. In crystalline silicates, Zr^{4+} ions have a coordination of 8, with each Zr-atom making *edge and corner connections* to SiO_4^{4-} tetrahedra.^{2,4} This same bonding coordination of 4 for Si and 8 for Zr(Hf) is assumed for the amorphous compound silicates.

The contribution of a vibrational mode to the dielectric constant is proportional to the square of its transverse infrared effective charge, e_T^* , and is different for different bonding coordinations of the same atom pair.^{9,13} The FTIR spectra of Fig. 2 indicate a broadening of the 950 cm^{-1} feature with increasing x . Based on Fig. 3, the broadening occurs at alloy concentrations where the Zr-atom coordination and ratio of *edge-* to *corner-connected* arrangements has increased. If e_T^* scaled directly with increases in the number of terminal Si–O bonds, this broadening would have been accompanied by a marked increase in absorbance of the 950 cm^{-1} feature relative to the network Si–O–Si spectral peak at 1065 cm^{-1} . To the contrary, FTIR results indicate the relative absorbance of terminal Si–O groups does not scale in this way, and

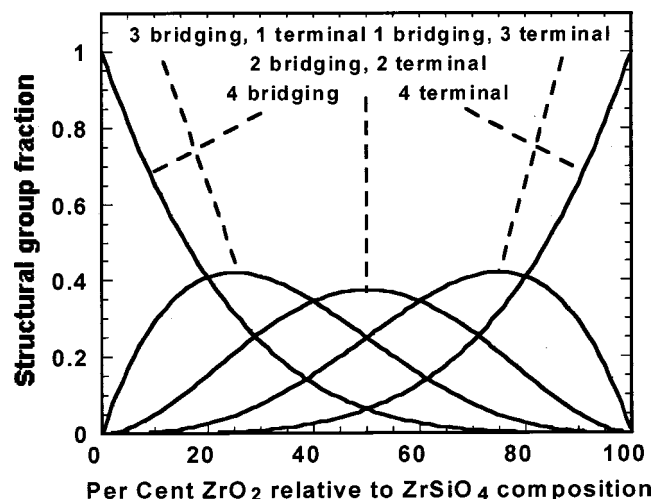


FIG. 4. Transition in local bonding arrangements of Zr atoms in Zr silicate alloys from low to high ZrO_2 concentrations. At low concentrations the dominant bonding arrangements are between the Zr atoms and four terminal O atoms in a *corner-connected* geometry. At higher concentrations (fraction of $\text{ZrO}_2 > 30\%$ – 35%), there is a transition to bonding including more than one O atom in *edge-connected* arrangements.

therefore the absorbance *decreases* with increasing Zr coordination. The *bond order* for a Zr–O bond is defined as the ratio of number of valence electrons available from each Zr atom (4) to the number of O-atom nearest-neighbors. Based on this definition, four-fold coordinated Zr atoms have the largest bond order, 1. They also have the highest degree of covalency,¹² so that dynamic contributions to e_T^* are larger than for higher bonding coordinations in which bond order is reduced and bonding becomes more ionic.^{9,13} Scaling of local properties such as bond energies and stretching force constants with bond order is well established.¹² Consistent with the relative absorption strengths of single, double, and triple carbon-oxygen bonds, this scaling can be extended to e_T^* . Since the contributions of infrared active modes to k are proportional to $(e_T^*)^2$, the appropriate scaling variable is the square of the bond order. There is also an additional and smaller contribution to the dielectric constant from electronic transitions that is included in the end-member constants of the scaling relationship given later.

Based on Eq. (1) and an assumption that contribution of Zr–O bonds to the dielectric constant scales quadratically with Zr–O bond order, the variation of k with alloy composition is approximated by

$$k \sim 3.9w^4 + 12(4a_{1,3}zw^3 + 6a_{2,2}z^2w^2 + 4a_{3,1}z^3w + a_{4,4}z^4), \quad (2)$$

where the first term is the contribution to k from Si–O–Si bonding, and the second term is from Si–O–Zr bonding. The constants 3.9 and 12 fix the end-member values.^{1,4} Combining Eq. (2) with Eq. (1), the following relationship is obtained:

$$k \sim 3.9 + 8.1(4a_{1,3}zw^3 + 6a_{2,2}z^2w^2 + 4a_{3,1}z^3w + a_{4,4}z^4); \quad (3)$$

$a_{i,j}$ are the product of (i) the number of terminal Si–O bonds per group, and (ii) the square of an average bond order. The $a_{i,j}$'s are approximated by $a_{1,3} \sim 1x(4/4)^2 = 1$, $a_{2,2} \sim 2x[4/(5-6)]^2 \sim 1.05$, $a_{3,1} \sim 3x[4/(6-7)]^2 \sim 1.15$, and $a_{4,4} \sim 4x(4/8)^2 = 1$, and are of order 1. The curve in Fig. 1 is for $a_{i,j} = 1$. Values of $a_{2,2}$ and $a_{3,1} > 1$ would increase k for alloys with more than 45%–50% ZrO₂ relative to ZrSiO₄ (or $x > 0.25$). Since values of k for Zr(Hf) content > 7 at. % have not been reported, the application of the model is restricted to alloys with lower concentrations. The experimental data from Refs. 1, 3, 4, and 5 with alloy content < 7 at. % Zr fall close to calculated curve indicating that the empirical relationship of Eq. (3) provides a quantitative description of enhanced dielectric constants for alloys in this composition range. A similar enhancement in the index of refraction, or equivalently the optical frequency dielectric constant, is also expected to occur in low Zr(Hf) content silicate alloys. Our initial experiments have indicated that this enhancement is present, and that it also scales with the square of the bond order. In the spirit of the analysis presented above, this contribution is *implicitly included* in the constant and $a_{i,j}$ terms of Eq. (3).

It has been shown that the enhanced dielectric constants of the SiO₂-rich Zr and Hf silicates are due primarily to the

four-fold coordination of the Zr(Hf) atoms in the alloy composition range below about 7 at. %. Similar enhancements in k at low metal-atom concentrations are also expected for SiO₂-rich silicate alloys with (i) TiO₂, (ii) Y(La)₂O₃ for compositions up to the *first* silicate phase, La(Y)₂SiO₅,¹⁴ and (iii) oxides of other polarizable atoms such as Pb, Bi, Tl, etc. Chemical bonding at Si-silicate alloy interfaces should be similar to Si–SiO₂ interfaces, so that in addition to providing significantly increased capacitance and reduced direct tunneling, incorporation of these silicate alloys into MOS devices should yield interface properties and reliabilities similar to those of devices with SiO₂ dielectrics.

Note added in proof: As-deposited Zr silicate alloys with values of x from 0.1 to 0.8 were studied by extended x-ray absorption fine structure spectroscopy (EXAFS). Analysis of EXAFS data confirmed the increases in Zr atom coordination with increasing ZrO₂ content that have been discussed in the text. The coordination of Zr increased from 4.5 ± 1 for an $x \sim 0.1$ (or ~ 3.3 at. % Zr) alloy to 7.2 ± 1 for samples with $x \sim 0.25$ (or ~ 8.3 at. % Zr), spanning the range in which the dielectric constant enhancement is decreasing (see Fig. 1). In addition, analysis of the EXAFS data indicated two Zr–O nearest neighbor distances of 0.21 and 0.23 nm, approximately equal to the two Zr–O bond-lengths in the crystalline ZrSiO₄ phase.

This research is supported by the NSF, ONR, AFOSR, and the SEMATECH/SRC Front End Processing Center. One of the authors (G.L.) acknowledges a discussion with Professor W. A. Harrison of Stanford University, relative to model calculations for transverse effective charges. In addition, the authors acknowledge helpful discussions with Professor D. E. Aspnes, Professor J. R. Hauser, Professor A. Kingon, Professor J. P. Maria, Professor V. Misra, and Professor G. N. Parsons, all of North Carolina State University. Finally, Professor D. Sayers and Weiqing Zhou are acknowledged for their assistance with the EXAFS studies.

¹G. D. Wilk and R. M. Wallace, Appl. Phys. Lett. **74**, 2854 (1999).

²D. Wolfe, K. Flock, R. Therrien, B. Rayner, L. Günther, N. Brown, B. Claffin, and G. Lucovsky, Mater. Res. Soc. Symp. Proc. **567**, 343 (1999).

³G. D. Wilk, R. M. Wallace, and J. M. Anthony, J. Appl. Phys. **87**, 484 (2000).

⁴G. D. Wilk and R. M. Wallace, Appl. Phys. Lett. **76**, 112 (2000).

⁵V. Misra (unpublished).

⁶N. Jayasundere and B. V. Smith, J. Appl. Phys. **73**, 2462 (1993).

⁷G. Rayner, R. Therrien, and G. Lucovsky, Mater. Res. Soc. Symp. Proc. (in press).

⁸R. Zallen, *The Physics of Amorphous Solids* (Wiley, New York, 1983), pp. 49–59.

⁹W. A. Harrison, *Elementary Electronic Structure* (World Science, Singapore, 1999), Chap. 11.

¹⁰J. C. Phillips, J. Vac. Sci. Technol. B **18**, 1749 (2000).

¹¹R. Zallen, *The Physics of Amorphous Solids* (Wiley, New York, 1983), pp. 100–101.

¹²F. A. Cotton and G. Wilkenson, *Advanced Inorganic Chemistry*, 3rd ed. (Wiley, New York, 1972), pp. 122–124.

¹³E. Burstein, M. H. Brodsky, and G. Lucovsky, Int. J. Quantum Chem. **1s**, 759 (1967).

¹⁴N. A. Torpov and I. A. Bondar, Izv. Akad. Nauk SSSR, Otd. Khim. Nauk **4**, 547 (1961).